iScience

CellPress
OPEN ACCESS

Article

Protein degradation of Lsd1 is mediated by Bre1 yet opposed by *Lsd1-interacting lncRNAs* during fly follicle development

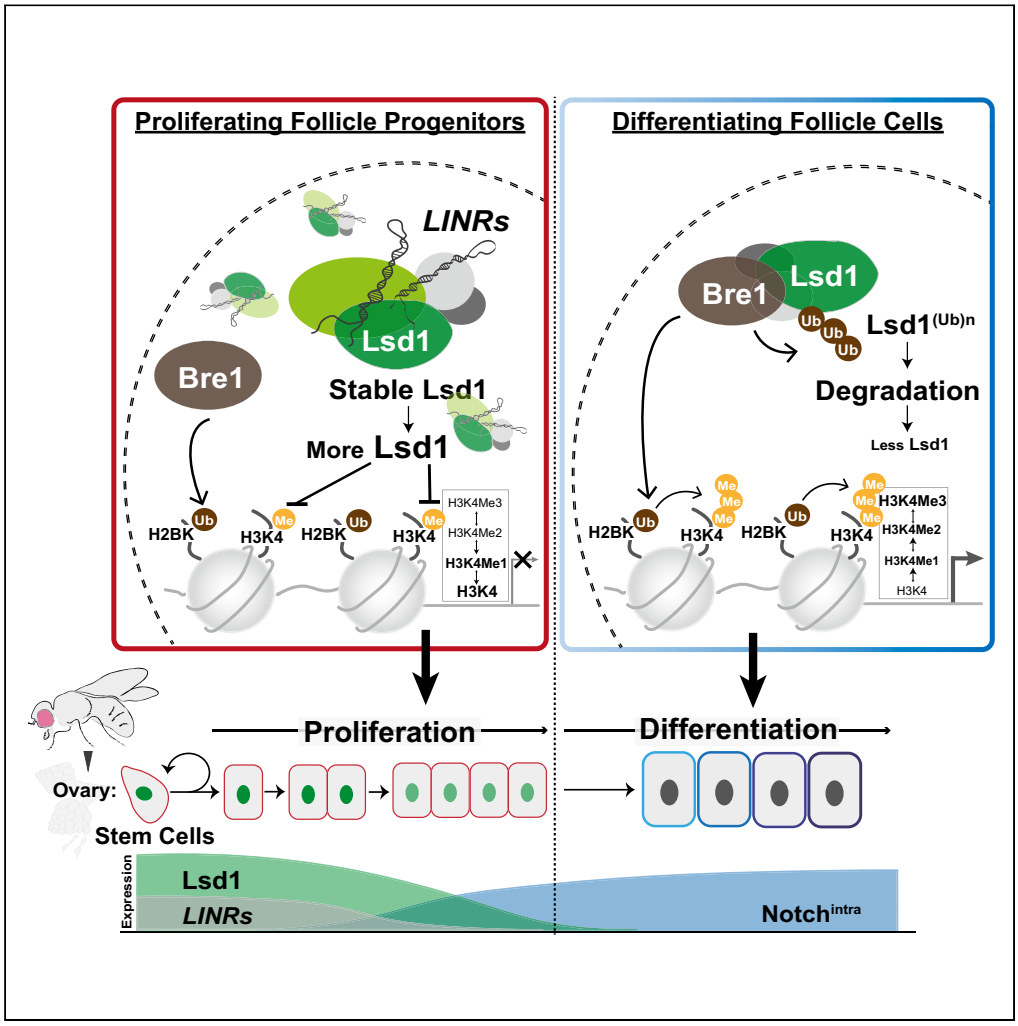

Chun Ting Lin, Ruei-Teng Ting, Yang-Hsuan Ou, Tzu-Ling Shao, Ming-Chia Lee

lee.mingchia@nycu.edu.tw

Highlights

Lsd1 protein expression is tuned post-translationally during fly follicle development

Bre1 is an E3 ligase that mediates Lsd1 protein degradation

Bre1 ubiquitinates Lsd1 to underlie follicle progenitor differentiation

Bre1-mediated Lsd1 degradation is opposed by Lsd1-interacting lncRNAs

Lin et al., iScience *27*, 109683
May 17, 2024
https://doi.org/10.1016/j.isci.2024.109683

iScience

CellPress
OPEN ACCESS

Article

Protein degradation of Lsd1 is mediated by Bre1 yet opposed by *Lsd1-interacting lncRNAs* during fly follicle development

Chun Ting Lin,[1,2,3] Ruei-Teng Ting,[1,2,3] Yang-Hsuan Ou,[1,2] Tzu-Ling Shao,[1,2] and Ming-Chia Lee[1,2,4,*]

SUMMARY

Tissue development, homeostasis, and repair all require efficient progenitor expansion. Lysine-specific demethylase 1 (Lsd1) maintains plastic epigenetic states to promote progenitor proliferation while over-expressed Lsd1 protein causes oncogenic gene expression in cancer cells. However, the precise regulation of Lsd1 protein expression at the molecular level to drive progenitor differentiation remains unclear. Here, using *Drosophila melanogaster* oogenesis as our experimental system, we discovered molecular machineries that modify Lsd1 protein stability *in vivo*. Through genetic and biochemical analyses, an E3 ubiquitin ligase, Bre1, was identified as required for follicle progenitor differentiation, likely by mediating Lsd1 protein degradation. Interestingly, specific Lsd1-interacting long non-coding RNAs (*LINRs*) were found to antagonize Bre1-mediated Lsd1 protein degradation. The intricate interplay discovered among the Lsd1 complex, *LINRs* and Bre1 provides insight into how Lsd1 protein stability is fine-tuned to underlie progenitor differentiation *in vivo*.

INTRODUCTION

Tissue development requires programmed cell differentiation with temporospatial precision. Dynamic modifications on chromatin landscape underlie transcriptomic changes that direct cellular differentiation. Alterations of such epigenetic regulation likely cause tissue malfunction and diseases.[1–4] Lysine-specific demethylase 1 (Lsd1) was among key epigenetic modifiers identified that regulate differentiation of stem/progenitor cells while its dysregulation tightly associates with tumorigenesis.[5] As the first histone demethylase discovered, conserved structure and function of Lsd1 have been thoroughly documented among eucaryotes.[6–8] The aberrant Lsd1 expression was found in various types of cancer. Specifically, elevated Lsd1 protein expression has been discovered in poorly differentiated neuroblastoma, sarcoma, neuroendocrine carcinomas, breast cancer, lung cancer, colon cancer, and ovarian cancer cells.[9–13] Growing studies implicating the pivotal role of Lsd1 in cancer development/progression have prompted the idea of utilizing Lsd1 as a therapeutic target for cancer interventions.[6,8,14,15] The carcinogenic property of Lsd1 may be explained by its diverse function implicated in controlling key cellular processes. Specifically, as a histone demethylase, Lsd1 binds monomethylated or dimethylated lysine residues to oxidize the methyl group with its conserved flavin-dependent monoamine oxidase domain. When Lsd1 partners with CoRest, CtBP, or NuRD to form corepressor complexes that remove the methyl group at H3K4 residues, Lsd1 suppresses the expression of lineage-specific genes.[16,17] On the other hand, Lsd1 recognizes and demethylates methylated H3K9 when it associates with nuclear receptors for activating gene expression.[16,17] Moreover, Lsd1 was reported to demethylate non-histone substrates to modify the function of two key tumor suppressor genes. Lsd1 catalyzes p53 demethylation to directly modulate p53 function, while Lsd1 demethylates E2F1 and MYPT1 to modify their binding to Rb protein and affects Rb activity indirectly.[16,17] Furthermore, the association between Lsd1 and specific long non-coding RNAs (lncRNAs) was recently reported to account for specific tumorigenic gene expression.[16,18,19] Taken together, multiple key cellular processes are likely simultaneously affected by elevated levels Lsd1 protein expression to underlie tumorigenesis. However, the molecular mechanisms of how Lsd1 protein levels are precisely tuned to ensure normal cellular physiology remain largely unknown.

Notably, the Lsd1 function is modified by specific posttranslational modifications. For instance, methylation at a conserved lysine residue (K^{322}) was found to stabilize Lsd1 protein expression potentially by affecting its polyubiquitination.[17,20] The idea that Lsd1 protein stability is dynamically regulated to underlie cellular differentiation is further supported by several recent studies. For instance, an E3 ligase Jade-2 was reported to de-stabilize Lsd1 protein during neuronal differentiation, although Jade-2 contains no classic RING domain that was commonly found in canonical E3 ligases for catalyzing protein polyubiquitination.[21] In addition, specific deubiquitylases (e.g., USP28 and USP7) have

[1]Department of Life Sciences and Institute of Genome Sciences, National Yang Ming Chiao Tung University, Taipei, Taiwan
[2]Info & Research Bldg, Rm 904, #155, Sec. 2, Li-Nong St, Taipei City 112, Taiwan
[3]These authors contributed equally
[4]Lead contact
*Correspondence: lee.mingchia@nycu.edu.tw
https://doi.org/10.1016/j.isci.2024.109683

been shown to be highly expressed in cancer cells for stabilizing Lsd1 protein expression,[22,23] although the bona fide E3 ligases responsible for Lsd1 ubiquitination in these cancer cells remain unclear. These findings present an attractive model that Lsd1 protein stability is dynamically controlled through ubiquitination to affect Lsd1-dependent epigenetic regulations. However, this model has not been fully investigated *in vivo*.

Drosophila oogenesis provides a great system for studying epithelial progenitor growth and differentiation *in vivo*. During fly oogenesis, each developing ovarian follicle represents a highly reproducible system of cellular differentiation in miniature. The over 800 follicle cells that cover individual egg chambers as a monolayer epithelium are derived from two follicle stem cells (FSCs). Two FSCs undergo asymmetrical cell division, producing daughter cells that then undergo rounds of mitosis to amplify the number of follicle cells. These dividing follicle cells (i.e., follicle progenitors) respond to induction cues with temporospatial precision to result in a sequential production of distinct follicular cell types, contributing to the formation of an egg's internal structure and protective shell. For example, the differentiation of main body follicle cells occurs at stage 6 egg chambers, when follicle progenitors activate Notch signaling to cease mitosis and to enter endocycle (M-E transition) in response to germline-expressing Delta.[24–29] Notably, Lsd1 plays a cell-specific role in supporting fly oogenesis. Lsd1 regulates early somatic cell differentiation to affect the niche of germline stem cells (GSCs). Moreover, Lsd1 acts autonomously in follicle progenitors to promote their expansion.[25,30–34] Interestingly, in follicle progenitors, the gradually reduced Lsd1 protein levels coincide with the occurrence of M-E transition.[25] Furthermore, our recent discovery of Lsd1-interacting non-coding RNAs (*LINRs*) reveals collaborative efforts of Lsd1 and lncRNAs in regulating ovarian cell differentiation and suggests that RNA-mediated modulations on Lsd1 function may be preserved through evolution.[35] Given the conserved role of Lsd1 documented in regulating cell differentiation, here we use *Drosophila* oogenesis as our *in vivo* system to investigate how cellular Lsd1 protein expression is controlled. We discovered that Lsd1 protein stability is regulated by ubiquitin-proteasome system (UPS) during fly follicle development. Through genetic and biochemical means, an E3 ligase, Bre1, was identified to mediate Lsd1 protein degradation during follicle cell differentiation. Interestingly, the interaction between Bre1 and Lsd1 was enhanced upon hydrolysis of double-stranded RNAs (dsRNAs) and suppressed by the presence of *LINR-2* transcripts *in vitro*. Consistently, reduced Lsd1 protein expression was detected in both *LINR-1* and *LINR-2* mutant ovaries, indicating that specific *LINRs* interfere with the binding between the Lsd1 complex and Bre1, allowing stable Lsd1 protein expression. The intricate interplay we discovered among the Lsd1 complex, *LINRs*, and Bre1 reveals how Lsd1 protein stability is fine-tuned to regulate follicle progenitor differentiation *in vivo*.

RESULTS

Lsd1 protein levels are regulated through ubiquitin-dependent degradation during fly oogenesis

In follicle cells, stage-dependent expression of Lsd1 protein is evident during fly follicle development (Figure 1A, and a study by Lee and Spradling[25]). The levels of Lsd1 protein start high in early follicle progenitors but are down-regulated in follicle cells that undergo M-E transition at stage 6 egg chambers. Interestingly, similar levels of follicular Lsd1 transcripts visualized by single molecule fluorescence *in situ* hybridization (Figures 1B and 1C) suggest that the stage-dependent Lsd1 protein expression may not be explained by transcriptional regulation. Therefore, to test if ovarian Lsd1 protein expression is modified posttranslationally, we monitored ovarian Lsd1 protein expression while blocking protein synthesis using cycloheximide. Interestingly, ovaries treated with cycloheximide for 4 h showed decreased levels of Lsd1 protein expression (Figure 1D), indicating that newly synthesized ovarian Lsd1 protein undergoes degradation within a few hours. We then utilized a proteasome inhibitor MG132 to determine if ovarian Lsd1 protein degradation requires proteasome activity. Given that MG132 treatment for 2 h was sufficient to increase the levels of ovarian Lsd1 protein detected by both western blotting (by about 2-fold; Figures 1E and 1F) and immunostaining (Figure S1) and also to increase the amount of polyubiquitinated Lsd1 ($Lsd1^{Ub}$) (Figure 1G), specific UPS machineries are likely involved in regulating ovarian Lsd1 protein degradation.

Identification of ovarian E3 ubiquitin ligases that affect Lsd1 protein expression in follicle progenitors

Protein ubiquitination requires concerted action among ubiquitin-activating enzymes (E1s), ubiquitin-conjugating enzymes (E2s), and ubiquitin ligases (E3s) (Figure 2A). Because ubiquitin E3 ligases are responsible for substrate recognition, the identification of Lsd1-specific E3 ligase(s) is key to understanding how Lsd1 protein stability is specifically regulated at the molecular level. To identify candidate E3 ligases that modify Lsd1 protein stability in follicle progenitors, a powerful clonal analysis system, FLP-OUT assay, was utilized. Briefly, at single follicle progenitors where flipase (FLP) expression is induced upon heat shock, the excision of FRT-flanked STOP cassette is mediated by FLP to allow the expression of GAL4. Then, GAL4 expression drives transcription of both green fluorescent protein (GFP) and specific short hairpin RNAs (shRNAs) within these GAL4-expressing clones (each includes the initial FLP-OUT cell and its progenies; Figure 2B). Clones located within stage 3–6 egg chambers were examined to identify E3 ligases that act in follicle progenitors modifying Lsd1 protein expression. Supposedly, knockdown of Lsd1-specific E3 ligases will lead to accumulation of cellular Lsd1 protein (Figure 2C). Among the 11 RNAi line of seven E3 ligases examined (i.e., *Bre1*, *gzl*, *Hecw*, *HUWE1*, *Prp191*, *mus302*, and *Mkrn1*), knockdown of Bre1 successfully led to cellular accumulation of Lsd1 protein in follicle cells of stage 3–6 egg chambers (Figure 2D), indicating that Bre1 functions to negatively regulate Lsd1 protein expression in follicle progenitors. Bre1, a RING domain containing E3 ubiquitin ligase, is previously known for its well conserved function of mediating mono-ubiquitination on histone 2B (H2B).[36–38] Interestingly, we noticed that in the *Bre1* knockdown (*Bre1*-KD) follicle cells the elevated Lsd1 protein expression was sometimes accompanied by altered patterns of nuclear DAPI staining (Figure S2A). Specifically, the signals of DAPI staining appear to be more diffused yet occupy a larger area in the *Bre1*-KD follicle cells. However, even though the patterns of

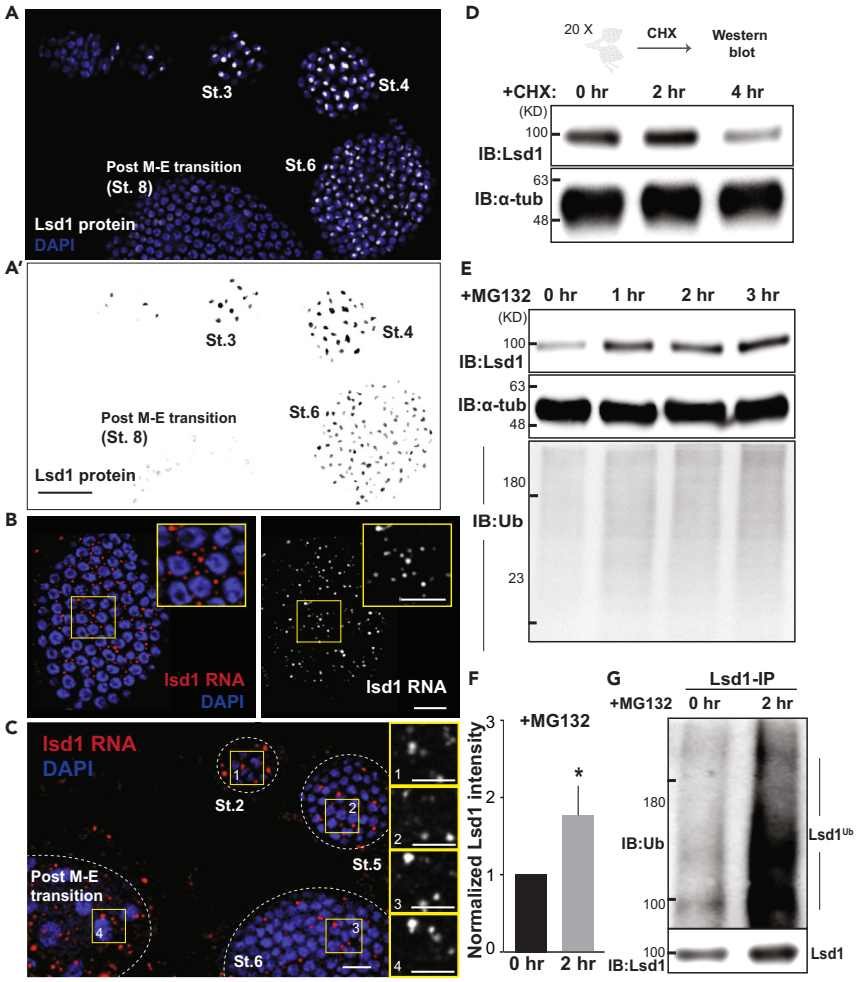

Figure 1. Lsd1 protein levels are regulated through ubiquitin-dependent degradation during fly oogenesis

(A) Lsd1 protein in follicle cells shows a stage-dependent expression profile during follicle development. Early follicle progenitors (at stage 2 [St.2] egg chambers) express higher levels of Lsd1 protein, while reduced follicular Lsd1 protein expression is seen in stage 6 (St.6) and later chambers (post M-E transition). To better visualize the stage-dependent expression profile of Lsd1 protein, in (A'), signals of Lsd1 protein were shown in black (using ImageJ/Inverted LUT function) while the nuclei of individual follicle cells were outlined (in light gray) based on their nuclear DAPI signals.

(B) The cytoplasmic expression of Lsd1 transcripts was visualized in follicle cells by *in situ* hybridization (ACD BaseScope). Insets are the zoom-in pictures of regions outlined by yellow boxes.

(C) Visualization of Lsd1 transcripts in follicle cells of developing egg chambers. Different stages of egg chambers are sequentially labeled from stage 3 (St.3) to a post M-E transition egg chamber. Insets are the zoom-in pictures of four regions, each outlined with a yellow box that shows cytoplasmic Lsd1 RNAs.

(D) The levels of ovarian Lsd1 protein were determined at 0 h, 2 h, and 4 h post application of cycloheximide (CHX, 200 μM). The expression of α-tubulin was used as the loading control.

(E) Accumulation of ovarian Lsd1 protein was detected post MG132 (10 μM) application, which inhibits proteasome activity. The expression of α-tubulin was used as the loading control, while the expression of ubiquitin (IB: Ub) was used to monitor accumulation of ubiquitinated proteins post-MG132 treatment.

(F) MG132 treatment for 2 h led to a significant increase of ovarian Lsd1 protein levels (quantified from three independent experiments).

(G) When Lsd1-immunoprecipitation (Lsd1-IP) was performed and followed by immunoblotting against ubiquitin (IB: Ub), ubiquitinated Lsd1 ($Lsd1^{Ub}$) was detected 2 h post MG132 treatment. Scale bars: 20 μm. Scale bar in the insets: 5 μm. Error bars: standard errors. *$p < 0.05$; Student's t test.

DAPI staining are different, similar total intensities of DAPI signal were found between *Bre1*-KD (GFP+) cells and their neighboring (GFP−) control cells, indicates that the *Bre1*-KD follicle cells maintain normal DNA content (Figures S2B and S2C).

Lsd1 protein accumulation, in response to *Bre1* knockdown, delays follicle cell differentiation

Given that increased Lsd1 protein expression was detected in *Bre1* FLP-OUT clones generated using two independent RNAi lines ($Bre1^{RNAi\#1}$ and $Bre1^{RNAi\#2}$), Bre1 likely downregulates Lsd1 protein expression in a cell-autonomous manner (Figures 2D and 3A). As indicated by our quantifications, higher signal intensities of Lsd1 staining were detected in *Bre1*-KD cells relative to the non-clonal control cells, resulted in

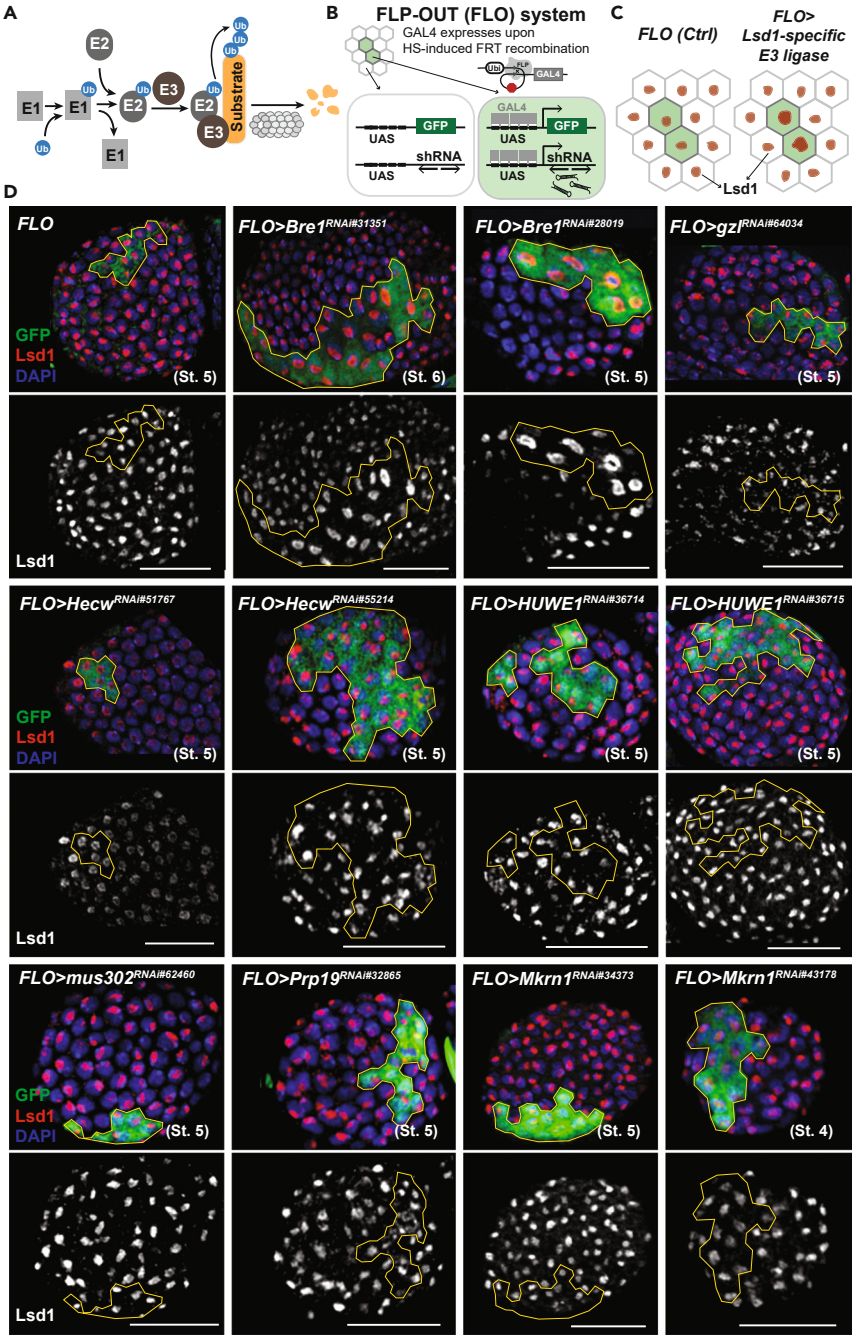

Figure 2. Identification of ovarian E3 ubiquitin ligases that affect Lsd1 protein expression in follicle progenitors

(A) A schematic of UPS-mediated protein degradation. Protein ubiquitination requires the concerted efforts among E1s, E2s,and E3s.

(B) A schematic illustrates that heat shock induces the expression of FLP to catalyze FLP-OUT (FLO) reaction (excision of CD2 stop cassette) and then cause GAL4 expression. In those FLO cells, GAL4 expression activates the transcription of GFP and shRNAs targeting specific E3 ligases.

(C) Knockdown of Lsd1-specific E3 ligase(s) by the FLO system predicts cellular accumulation of Lsd1 protein.

(D) Representative pictures of Lsd1 protein expression detected in egg chambers that contain GFP expressing FLO clones (yellow outlines). In addition to the FLO control, seven ovarian E3 ligases were examined using FLO-mediated gene knockdown assays. Among the 11 RNAi lines of seven E3 ligases (*Bre1*, *gzl*, *Hecw*, *HUWE1*, *Prp191*, *mus302*, and *Mkrn1*) tested, knockdown of Bre1 expression with two RNAi lines (*Bre1*$^{RNAi\#31351}$ and *Bre1*$^{RNAi\#28019}$) led to increased Lsd1 protein expression. Scale bars: 20 μm.

CellPress
OPEN ACCESS

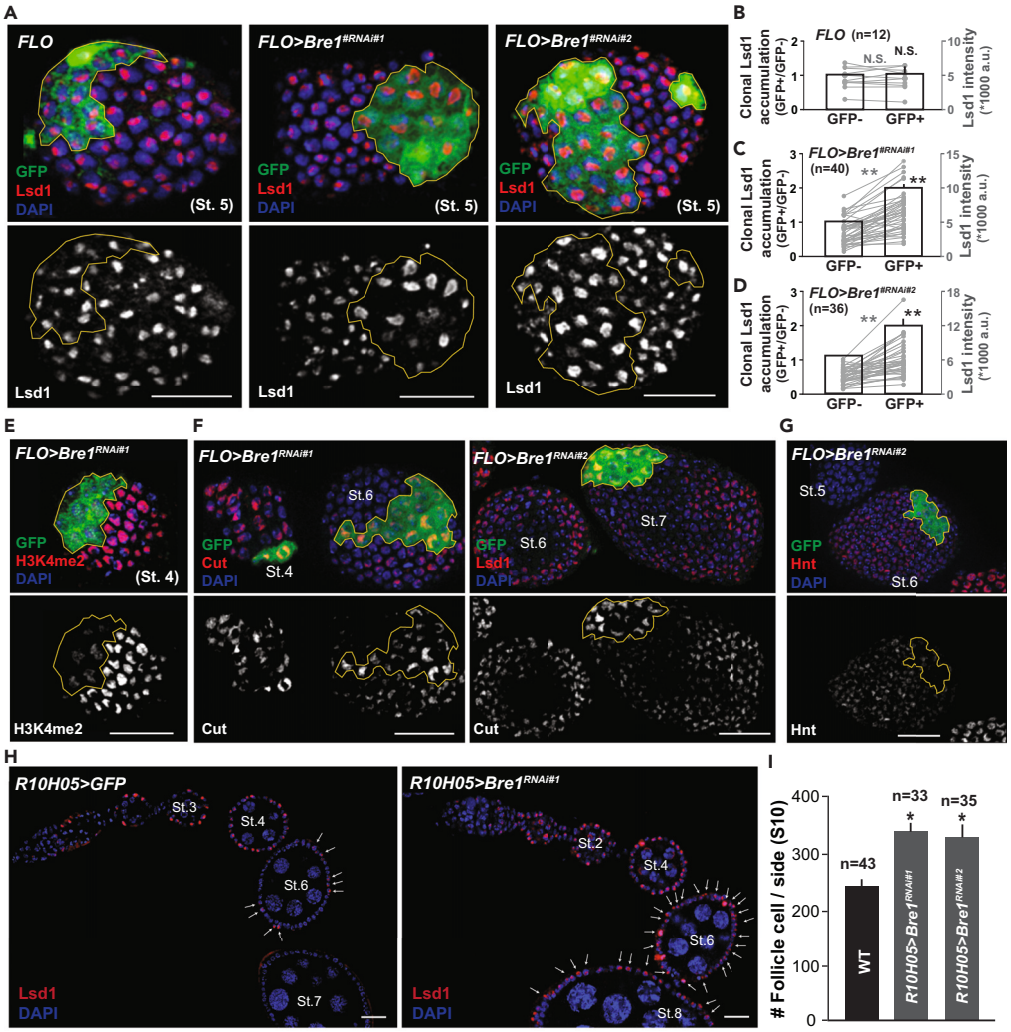

Figure 3. Lsd1 protein accumulation, in response to *Bre1* knockdown, delays follicle cell differentiation

(A) Clonal accumulation of Lsd1 protein was observed in the FLO clones (yellow outlines) of *Bre1* knockdown using $Bre1^{RNAi\#31351}$ ($Bre1^{RNAi\#1}$) and $Bre1^{RNAi\#28019}$ ($Bre1^{RNAi\#2}$) lines.

(B) Similar levels of Lsd1 protein expression were detected in control FLO clones.

(C and D) Among forty FLO $Bre1^{RNAi\#1}$ clones and thirty-six FLO $Bre1^{RNAi\#2}$ clones examined (in stage 3–7 egg chambers), about a 2-fold increase in clonal accumulation of Lsd1 protein was observed in *Bre1*-KD (GFP+) cells when compared to the neighboring cells (GFP−). The intensity of Lsd1 (left y axis) indicates the average levels of Lsd1 protein in GFP+ and GFP− cells (a pair of gray circles connected by a line) for each FLO *Bre1*-KD clone.

(E) Upon *Bre1* knockdown, reduced H3K4Me2 signals were observed compared to neighboring cells.

(F) *Bre1* knockdown follicle cells (yellow outlines) retain higher Cut expression at stage 6 (St. 6) and stage 7 (St.7) egg chambers.

(G) The *Bre1*-KD follicle cells (yellow outlines) showed delayed hindsight (Hnt) expression at stage 6 (St. 6).

(H) Knocking down *Bre1* in follicle cells ($R10H05>Bre1^{RNAi\#1}$ and $R10H05>Bre1^{RNAi\#2}$) led to elevated and prolonged Lsd1 expression, as indicated by arrows showing cellular Lsd1 expression in stage 6 egg chambers and beyond, compared to control ovarioles (*R10H05>GFP*). The increased Lsd1 protein expression is accompanied with an increased number of total follicle cells (quantified in (I)). Scale bars: 20 μm. Data shown in (B–D) and (I) were done by imaging/analyzing samples for each condition with at least 3 independent experiments. Data were presented as mean ± S.E. (standard errors). Student's t test was used to examine "Clonal Lsd1 accumulation" while paired Student's t test was used to examine the differences of Lsd1 intensity among individual clones. $^{**}p < 0.01$; N.S., non-significant.

~2-fold increases in clonal Lsd1 accumulations (Figures 3B–3D). Consistently, the results show that heterozygous *Bre1* mutant ovaries ($Bre1^{01640}/+$) contain a higher level of Lsd1 protein, and the exact *Bre1* mutant allele was able to partially restore the lower Lsd1 protein expression in *Lsd1* heterozygous mutant ovaries ($Lsd1^{4N}/+$), again supporting the idea that Bre1 acts to negatively regulate ovarian Lsd1 protein expression (Figure S3A). To determine the impacts of elevated Lsd1 protein expression on H3K4 methylation at single cells, we examined the levels of cellular H3K4me2, one of Lsd1's histone substrates. Lower intensities of H3K4me2 staining were observed in the *Bre1*-KD clones (Figure 3E), likely caused by the increased cellular Lsd1 protein expression. Interestingly, while H3K27Ac (a histone mark associated with active

chromatin state) was unaffected in the *Bre1*-KD cells, the increased levels of a repressive epigenetic mark, H3K27me3, suggest changes in histone methylation profiles of these *Bre1*-KD cells (Figure S3B). Furthermore, given that Lsd1 has been shown to promote follicle progenitor proliferation and delay M-E transition,[25] we determined whether Lsd1 protein accumulation in follicle cells affects their timing of undergoing M-E transition. The expression of Hindsight (Hnt) and Cut protein in follicle cells was utilized as molecular markers to indicate the onset of M-E transition.[28,29] As a result, in stage 6 egg chambers, *Bre1*-KD follicle cells seem to retain a higher level of Cut protein expression while showing delayed Hnt induction (Figures 3F and 3G), suggesting a somewhat delayed M-E transition in *Bre1*-KD follicle cells. We then took advantage of a follicle cell specific driver for knocking down *Bre1* expression in the entire follicle cell lineage (*R10H05>Bre1*$^{RNAi\#1}$). As shown in Figure 3H, *Bre1* knockdown led to elevated and prolonged Lsd1 protein expression in follicle cells, accompanied by an increased number of total follicle cells (Figure 3I). The results suggest that Bre1 lowers Lsd1 expression to allow timely follicle progenitor differentiation.

Bre1 regulates Lsd1 protein degradation through ubiquitination

To investigate whether impaired Lsd1 protein degradation autonomously underlies increased Lsd1 protein expression in the *Bre1*-KD cells, we tested if the clonal accumulation of Lsd1 is affected by MG132 application. We found that inhibition of proteasome activity globally (by MG132) was able to reduce the differential Lsd1 protein expression observed between the *Bre1*-KD and their neighboring cells (Figures 4A, 4B, and S4A). This indicates that Bre1 regulates Lsd1 protein expression thorough affecting its proteasome-mediated protein degradation. Furthermore, we examined if Bre1 is biochemically capable of mediating Lsd1 polyubiquitination. As shown in Figure 4C, we found that purified GST-Lsd1 was polyubiquitinated when incubated for 3 h with crude ovarian lysate plus HA-ubiquitin (HA-Ub) (see STAR Methods for a detailed protocol). This suggests that the ovarian lysate contains specific UPS machineries that are sufficient for catalyzing Lsd1 ubiquitination. Interestingly, when we substituted ovarian lysate with the Bre1 protein complexes immunoprecipitated from ovarian lysate (Bre1-IP), but not with lysate depleted with the Bre1 complexes (Bre1_del; Figure S4B), signals of polyubiquitinated Lsd1 were readily detected. These results support the model that the Bre1 complexes are required and capable of ubiquitinating GST-Lsd1 protein *in vitro*. Taken together, these findings indicate the capability of Bre1 to act as an E3 ligase, thereby mediating Lsd1 protein degradation.

Specific *LINRs* interfere with the binding between Lsd1 and Bre1 complexes to maintain stable Lsd1 protein expression

The idea that Bre1 acts as an Lsd1-specific E3 ligase is further supported by the physical interaction detected between Lsd1 and Bre1 using co-immunoprecipitation (co-IP) assays (Figures 5A and S5A). Recently, three long hairpin RNAs (lhpRNAs) were identified to associate with Lsd1 and to regulate fly oogenesis.[35] Thus, we investigated whether any of these *LINRs* are involved in modulating Lsd1 protein stability. Interestingly, the removal of dsRNAs, including *LINR-1-3*, by RNase III application specifically increased the amount of Lsd1 protein co-immunoprecipitated with Bre1 (Figures 5A and S5B). This result suggests that *LINR-1-3* or specific dsRNAs interfere with the Lsd1/Bre1 binding and affect Lsd1 protein stability. Indeed, reduced Lsd1 protein expression was observed in *LINR-1* and *LINR-2* mutant ovaries (*LINR-1*$^{\Delta}$ and *LINR-2*$^{\Delta}$, respectively; Figure 5B), confirming the requirement of *LINR-1* and *LINR-2* for maintaining stable ovarian Lsd1 protein expression. Notably, the expression of three ovarian *LINRs* was detected mainly during early oogenesis,[35] which coincided with the stage of oogenesis showing a higher level of Lsd1 protein expression. The model proposing that specific *LINRs* bind to Lsd1 complex to oppose Lsd1/Bre1 interaction predicts preferential incorporation of certain *LINRs* in the Lsd1 complexes but not within the Bre1 complexes. To investigate this, we carried out RNA immunoprecipitation (RIP) assays, specifically Bre1-RIP experiments, to determine the RNAs associated with Bre1 complex. Indeed, when compared to the average enrichment index of individual *LINRs* in our Lsd1-RIP datasets (Shao et al., 2022; [RPKM$^{Lsd1-RIP}$/RPKM$^{IgG-RIP}$]: *LINR-1* = 2.05 $\pm$ 0.87, *LINR-2* = 5.87 $\pm$ 0.92 and *LINR-3* = 2.55 $\pm$ 1.31) *LINR-1-3* were less enriched in the Bre1-RIP datasets ([RPKM$^{Bre1-RIP}$/RPKM$^{IgG-RIP}$]: *LINR-1* = 0.32 $\pm$ 0.09, *LINR-2* = 2.25 $\pm$ 2.41 and *LINR-3* = 0.86 $\pm$ 0.40) (Figures 5C and 5D). The fact that Bre1-IP was able to pull down Lsd1 (Figure 5A) but not *LINR-1-3* (Figures 5C and 5D) suggests that *LINRs*-bound Lsd1 complexes do not effectively interact with Bre1 for protein degradation. Furthermore, to specifically determine if the presence of *LINR-1* or *LINR-2* affects Lsd1/Bre1 binding and leads to stable Lsd1 protein expression, Bre1-IP experiments were performed in the presence of GFP, *LINR-1* or *LINR-2* RNAs (synthesized and folded *in vitro*). As shown in Figure 5E, the addition of *LINR-2* transcripts was sufficient to reduce the amount of Lsd1 protein pulled down by the Bre1 complexes. Moreover, reduced Lsd1 protein expression was observed in *LINR-2*$^{\Delta}$ mutant cells (Figures 5F and S5D). Taken together, our results support a model in which specific *LINRs* interact with Lsd1 complex to oppose Bre1-mediated Lsd1 protein degradation, allowing stable Lsd1 protein expression to facilitate follicle progenitor expansion (Figure 5G).

DISCUSSION

Here we use fly oogenesis as an *in vivo* system to uncover molecular machineries that modify Lsd1 protein stability to regulate follicle progenitor differentiation. Through FLP-OUT clonal assays, we have identified a ubiquitin E3 ligase, Bre1, which negatively regulates Lsd1 protein expression and impacts follicle progenitor differentiation (Figures 2, 3, and 4). Notably, our findings reveal that Bre1 regulates the degradation of Lsd1 protein in follicle progenitors (Figure 3I) and has the capability of catalyzing Lsd1 ubiquitination *in vitro* (Figure 4D). Intriguingly, this Bre1-mediated Lsd1 protein degradation process is likely modified by specific *LINRs*, particularly *LINR-2*, to maintain stable ovarian Lsd1 protein expression, underlies progenitor proliferation (Figure 5).

In this study, Bre1 was the sole E3 ligase that we discovered to modify Lsd1 protein expression among the seven ovarian E3 ligases tested (Figure 2). However, it is possible that additional Lsd1-specific E3 ligases may be uncovered through future genetic and biochemical screenings. Both Lsd1 and Bre1 are well-known histone modifiers that regulate chromatin states. Lsd1 catalyzes demethylation to reduce H3K4

CellPress
OPEN ACCESS

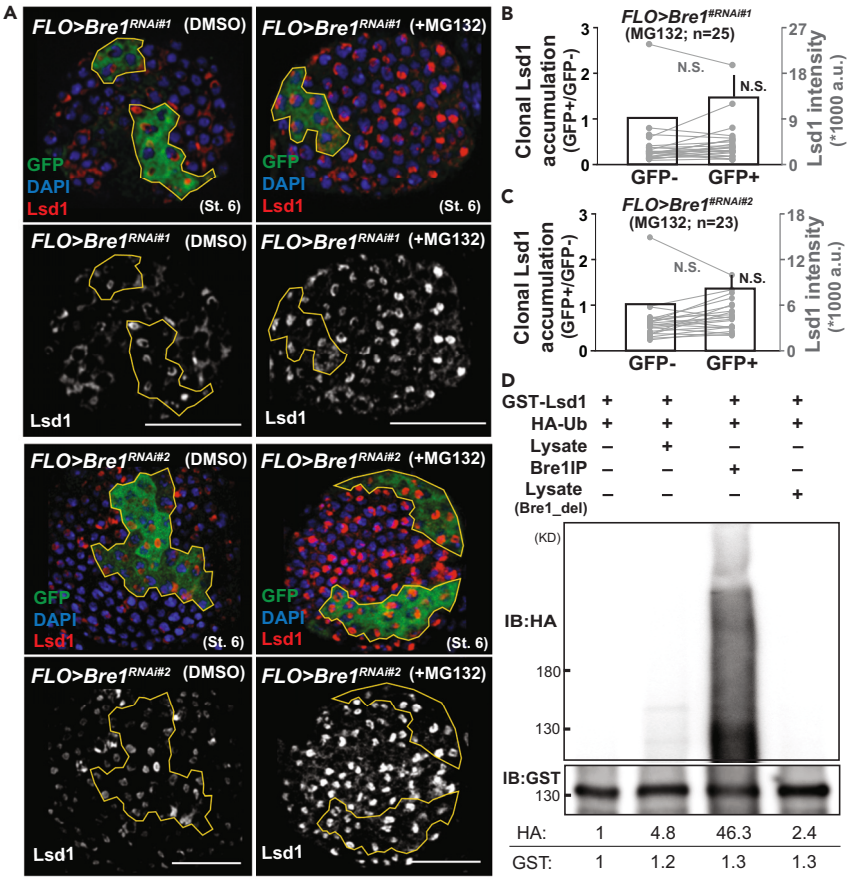

Figure 4. Bre1 regulates Lsd1 protein degradation through ubiquitination

(A) Compared to control (DMSO), less clonal accumulation of Lsd1 protein was observed in *Bre1*-KD cells (yellow outlines) after treating MG132 for 2 h.

(B and C) Among twenty-five FLO *Bre1*$^{RNAi\#1}$ clones and twenty-three FLO *Bre1*$^{RNAi\#2}$ clones examined, the application of MG132 for 2 h partially mitigated the clonal accumulation of Lsd1 protein in *Bre1*-KD cells. Consistently, in many *Bre1*-KD clones, Lsd1 intensity is no longer higher than the GFP- cells.

(D) To recapitulate ubiquitination on ovarian Lsd1 protein *in vitro*, purified GST-Lsd1 (0.5 μg) was mixed with crude ovarian lysate, HA-ubiquitin (HA-Ub) and ubiquitination buffer (containing ATP and MG132; see STAR Methods) for 3 h at room temperature. As a result, ubiquitination on GST-Lsd1 was detected using HA immunoblotting (IB: HA). Notably, robust signals of ubiquitinated Lsd1 were readily detected when ovarian lysate was substituted with the Bre1 protein complexes immunoprecipitated from ovarian lysate (Bre1-IP) but not the lysate depleted with Bre1 (Lysate Bre1_del). The same amount of GST-Lsd1 (IB: GST) was used in all four reactions. The normalized total signal intensity of anti-HA and anti-GST signals was presented. Scale bars: 20 μm. Data shown in (B and C) were done by imaging/analyzing samples for each condition with at least 3 independent experiments. Data were presented as Mean ± S.E. (standard errors). Student's t test was used to examine "Clonal Lsd1 accumulation" while paired Student's t test was used to examine the differences in Lsd1 intensity among individual clones. $^{**}p < 0.01$; N.S., non-significant.

methylation levels, thereby suppressing gene expression.[16,39,40] On the other hand, Bre1 encodes a RING finger-type E3 ligase that catalyzes monoubiquitination of histone H2B to promote nucleosome stabilization.[36–38,41–43] H2B ubiquitination (H2Bub) residing in the gene body has been found to serve as a hub in histone crosstalk, regulating Set1/COMPASS and Dot1 to respectively affect H3K4 and H3K79 methylation, thus underlining transcriptional elongation to promote gene expression.[38,44–47] Interestingly, H2Bub can also mediate gene silencing. Not only does H2Bub occurring at the promoter region suppress gene transcription, but H2Bub is also required to suppress the expression of antisense transcripts genome-wide and telomere-proximal genes.[42,43] The H2Bub-mediated regulations on nucleosome dynamics and gene expression suggests a key role of H2Bub in affecting chromatin structure. This may explain why an altered appearance of DAPI staining was observed in the Bre1 knockdown cells (Figure S2A). The idea that Bre1 acts as an Lsd1-specific E3 ligase aligns with their seemingly opposite roles in affecting H3K4 methylation. While future investigation is required, it is conceivable that Bre1 ensures stable and high levels of H3K4 methylation by both promoting the activity of H3K4 specific methyltransferase (Set1/COMPASS) and reducing the expression of a H3K4 demethylase (Lsd1). In addition, our findings may help explain why proteasome activity is required for efficient Bre1-mediated H3K4 methylation as previously indicated.[48] Considering recent reports that Bre1 generates chromatin-associated reaction chambers through a liquid-liquid phase separation mediated process for H2B ubiquitination during transcription,[49] it will be particularly intriguing to explore whether Bre1-containing condensates also play a role in modulating Lsd1 stability to affect local chromatin environments.

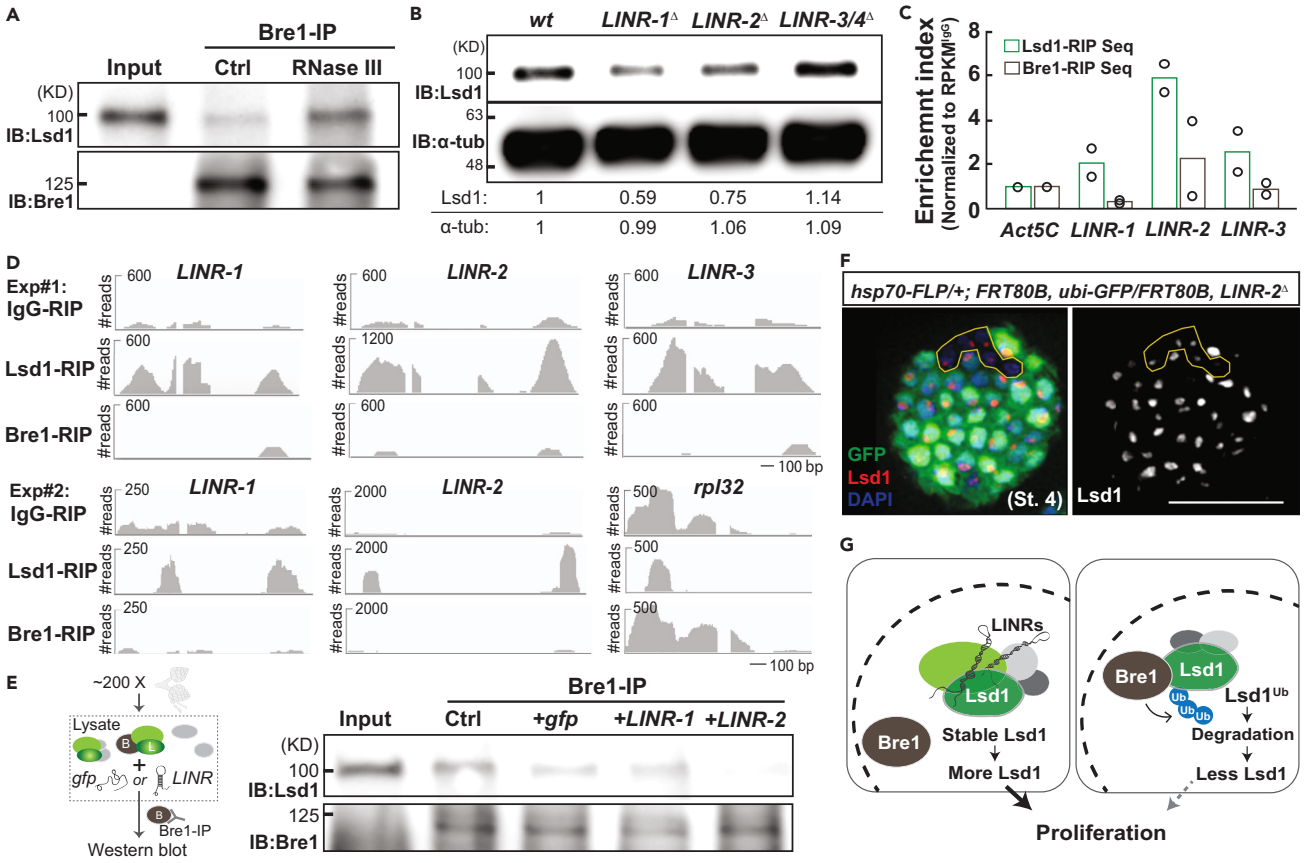

Figure 5. Specific *LINRs* interfere with the binding between Lsd1 and Bre1 complexes to maintain stable Lsd1 protein expression

(A) The binding between Lsd1 and Bre1 complexes was examined using Co-IP. Upon hydrolysis of double-stranded RNAs by RNase III treatment, the binding between Lsd1 and Bre1 complexes was enhanced.

(B) Reduced Lsd1 protein expression was detected in ovarian lysate prepared from young females of *LINR-1* and *LINR-2* deletion mutant flies (*LINR-1*$^{\Delta}$ and *LINR-2*$^{\Delta}$, respectively). The ovaries collected form young females are mainly composed of early-stage egg chambers (mostly before stage 8). The normalized total signal intensity of anti-Lsd1 and anti- α-tubulin was shown.

(C) From two independent Lsd1-RIP and Bre1-RIP experiments, the individual enrichment indexes of Act5C and three *LINRs* were indicated (circles). Averaged enrichment index of Lsd1-RIP ($RPKM^{Lsd1-RIP}/RPKM^{IgG-RIP}$, green bars) and Bre1-RIP ($RPKM^{Lsd1-RIP}/RPKM^{IgG-RIP}$, black bars) were shown.

(D) The read counts of individual *LINRs* and *rpl32* resulted from two sets of RIP experiment (i.e., IgG-RIP, Lsd1-RIP, and Bre1-RIP) are presented respectively.

(E) Experiments of Bre1-IP were performed when supplied with *in vitro* synthesized RNAs of GFP, *LINR-1*, or *LINR-2*, respectively.

(F) Reduced levels of Lsd1 protein expression were detected in *LINR-2*$^{\Delta}$ mutant cells.

(G) A schematic presenting the proposed model: In early progenitors, Lsd1 complexes bound by specific *LINRs* are stalely expressed to promote progenitor proliferation. Conversely, in late follicle progenitors, Lsd1 undergoes Bre1-mediated protein degradation in the absence of *LINRs*, allowing progenitor differentiation. Scale bars: 20 μm.

Even though the conserved structure and function of Bre1 as a H2B E3 ligase have been documented among eukaryotes, its two mammalian paralogues, RNF20 and RNF40, were shown to each poly-ubiquitinate non-histone substrates. While mouse RNF20 was found to poly-ubiquitinate Ebp1, an ErbB3 receptor-binding protein,[50] rat RNF40 has been shown to poly-ubiquitinate syntaxin to affect neuronal function.[51] Therefore, our identification of Bre1-mediated Lsd1 degradation likely presents the non-canonical yet conserved function of Bre1 in catalyzing poly-ubiquitination on non-histone substrates. Interestingly, different E2s were reported to help Bre1 in catalyzing specific protein ubiquitination. For instance, Ube2A/B (Rad6) collaborates with Bre1 to mediate H2B mono-ubiquitination, while Bre1 has been reported to work with Ube2E2 (UbcH8) for syntaxin poly-ubiquitination.[36,51,52] Given that the fly homologues of Ube2A (*ubc6*) and Ube2E2 (*CG5440*) were both found to express in ovarian somatic precursor cells (flybase), the exact UPS machineries that account for Bre1-mediated Lsd1 ubiquitination in follicle progenitors can be determined in future studies.

Our discovery that *LINRs*, especially *LINR-2*, stabilize ovarian Lsd1 protein expression, likely by influencing the assembly of specific Lsd1 complexes, helps explain the stage-dependent Lsd1 protein expression during follicle development. Given the higher expression levels of *LINRs* detected in early follicle progenitors,[35] it is conceivable that the presence of specific *LINRs* help stabilize Lsd1 protein autonomously to promote the expansion of early follicle progenitors. Further investigation is necessary to elucidate the regulatory function of individual

LINRs in shaping Lsd1 complex assembly at the molecular level. The recent identification of specific RNA-binding domains on Lsd1,[53] located within its SWIRM and amine oxidase domain, opens up the possibility of testing whether *LINRs* competitively interfere with Lsd1/Bre1 binding. Alternatively, given the binding between ovarian Lsd1 and CoRest is modulated by the presence of RNAs[35] and CoRest binding to Lsd1 is crucial for supporting Lsd1 H3K4 demethylase activity, complex assembly and protein stability,[54,55] it is of future interest to explore whether *LINRs* modify Lsd1/CoRest binding to indirectly impact the interaction between Lsd1 and Bre1. It is worth of noting that *LINR-2* appears to impact on Lsd1 protein expression in a dosage-specific manner. While here we showed reduced Lsd1 protein expression in *LINR-2*$^{\Delta}$ mutant ovaries (Figure 5B), an increased level of Lsd1 protein was found in the heterozygous *LINR-2*$^{\Delta}$ mutant (*LINR-2*$^{\Delta}$/+) ovaries, as previously indicated.[35] Such dosage-dependent impacts of *LINR-2* on Lsd1 protein levels may suggest a more sophisticated regulatory feedback loop mediated by *LINRs* on Lsd1 protein expression. Interestingly, our pilot chromatin immunoprecipitation (ChIP) experiments indicated the binding of Lsd1 and CoRest within the CoRest gene locus (data not shown). It is possible that *LINR-2* binds to Lsd1 not only to protect it from protein degradation but also to guide the complex to suppress CoRest gene expression. This model may explain why, in cases where half of the *LINR-2* dosage is missing, the Lsd1 complex fails to localize to the CoRest gene, leading to transcriptional activation of CoRest and stabilization of Lsd1 protein. However, in the absence of *LINR-2* entirely, despite CoRest transcriptional activation occurring, Lsd1 protein undergoes degradation by Bre1. Ultimately, the better understanding of how lncRNAs like *LINR-1* and *LINR-2* modulate Lsd1 protein stability could provide a molecular handle for manipulating Lsd1 protein expression to impact stem cell and progenitor differentiation *in vivo*.

Limitations of the study

Here, we use a candidate RNAi screen to identify Bre1, an E3 ligase, which negatively regulates Lsd1 protein stability, controlling follicle cell differentiation during fly oogenesis. However, considering that only 7 ovarian E3 ligases were tested in this study, it is possible that additional Lsd1-specific E3 ligases may be uncovered through systematic genetic and biochemical screenings in the future. On the other hand, although we found that immunoprecipitated Bre1 complexes were capable of mediating Lsd1 ubiquitination and ovarian lysate depleted with Bre1 complexes failed to ubiquitinate Lsd1 (Figure 4D), the exact UPS machineries associated with Bre1 and involved in Bre1-mediated Lsd1 ubiquitination remain unclear. Therefore, genetic analyses and corresponding *in vitro* ubiquitination assays are required to elucidate the composition of molecular machineries that mediate Lsd1 ubiquitination under physiological conditions.

STAR★METHODS

Detailed methods are provided in the online version of this paper and include the following:

- KEY RESOURCES TABLE
- RESOURCE AVAILABILITY
  - Lead contact
  - Materials availability
  - Data and code availability
- EXPERIMENTAL MODEL AND STUDY PARTICIPANT DETAILS
  - *Drosophila melanogaster* (Fruit fly)
- METHOD DETAILS
  - Fly husbandry
  - Generation of anti-Bre1 antisera
  - *In situ* hybridization
  - Immunoprecipitation and Western Blotting
  - Immunostaining and Microscopy
  - Clonal generation and measurements
  - RNA-Immunoprecipitation (RIP)
  - Generation and purification of GST-LSD1 recombinant protein
  - Ubiquitination assay
- QUANTIFICATION AND STATISTICAL ANALYSIS

SUPPLEMENTAL INFORMATION

Supplemental information can be found online at https://doi.org/10.1016/j.isci.2024.109683.

ACKNOWLEDGMENTS

We thank Allan Spradling and members of the Lee lab for their helpful discussions and comments on the project and manuscript. The RIP-seq experiments were conducted at the Genomics Center at National Yang Ming Chiao Tung University (MOST-110-2740-B-A49A). We appreciate the assistance from Taiwan Flycore, as well as the resources provided by Flybase and BDSC. This work was supported by Taiwan MOST/NSTC grants (107-2311-B-010 -001 -MY2, 108-2311-B-010 -001, and 109-2311-B-010 -004 -MY3) awarded to M.C.L.

AUTHOR CONTRIBUTIONS

C.T.L, R.-T.T., and M.-C.L. designed and performed the experiments. C.T.L, R.-T.T., and M.-C.L. analyzed the data. Y.-H.O. and T.-L.S. performed the experiments and analyzed the data. M.-C.L. wrote the paper.

DECLARATION OF INTERESTS

The authors declare no conflicts of interest.

Received: October 18, 2023
Revised: February 13, 2024
Accepted: April 4, 2024
Published: April 8, 2024

REFERENCES

1. Allis, C.D., and Jenuwein, T. (2016). The molecular hallmarks of epigenetic control. Nat. Rev. Genet. *17*, 487–500.
2. Dawson, M.A., and Kouzarides, T. (2012). Cancer epigenetics: from mechanism to therapy. Cell *150*, 12–27.
3. Iglesias-Bartolome, R., Callejas-Valera, J.L., and Gutkind, J.S. (2013). Control of the epithelial stem cell epigenome: the shaping of epithelial stem cell identity. Curr. Opin. Cell Biol. *25*, 162–169.
4. Cheng, Y., He, C., Wang, M., Ma, X., Mo, F., Yang, S., Han, J., and Wei, X. (2019). Targeting epigenetic regulators for cancer therapy: mechanisms and advances in clinical trials. Signal Transduct. Targeted Ther. *4*, 62.
5. Jones, P.A., Issa, J.P.J., and Baylin, S. (2016). Targeting the cancer epigenome for therapy. Nat. Rev. Genet. *17*, 630–641.
6. Ismail, T., Lee, H.K., Kim, C., Kwon, T., Park, T.J., and Lee, H.S. (2018). KDM1A microenvironment, its oncogenic potential, and therapeutic significance. Epigenet. Chromatin *11*, 1–15.
7. Gu, F., Lin, Y., Wang, Z., Wu, X., Ye, Z., Wang, Y., and Lan, H. (2020). Biological roles of LSD1 beyond its demethylase activity. Cell. Mol. Life Sci. *77*, 3341–3350.
8. Yang, C., Li, D., Zang, S., Zhang, L., Zhong, Z., and Zhou, Y. (2022). Mechanisms of carcinogenic activity triggered by lysine-specific demethylase 1A. Front. Pharmacol. *13*, 955218.
9. Hayami, S., Kelly, J.D., Cho, H.S., Yoshimatsu, M., Unoki, M., Tsunoda, T., Field, H.I., Neal, D.E., Yamaue, H., Ponder, B.A.J., et al. (2011). Overexpression of LSD1 contributes to human carcinogenesis through chromatin regulation in various cancers. Int. J. Cancer *128*, 574–586.
10. Lim, S., Janzer, A., Becker, A., Zimmer, A., Schüle, R., Buettner, R., and Kirfel, J. (2010). Lysine-specific demethylase 1 (LSD1) is highly expressed in ER-negative breast cancers and a biomarker predicting aggressive biology. Carcinogenesis *31*, 512–520.
11. Bennani-Baiti, I.M., Machado, I., Llombart-Bosch, A., and Kovar, H. (2012). Lysine-specific demethylase 1 (LSD1/KDM1A/AOF2/BHC110) is expressed and is an epigenetic drug target in chondrosarcoma, Ewing's sarcoma, osteosarcoma, and rhabdomyosarcoma. Hum. Pathol. *43*, 1300–1307.
12. Magerl, C., Ellinger, J., Braunschweig, T., Kremmer, E., Koch, L.K., Höller, T., Büttner, R., Lüscher, B., and Gütgemann, I. (2010). H3K4 dimethylation in hepatocellular carcinoma is rare compared with other hepatobiliary and gastrointestinal carcinomas and correlates with expression of the methylase Ash2 and the demethylase LSD1. Hum. Pathol. *41*, 181–189.
13. Schulte, J.H., Lim, S., Schramm, A., Friedrichs, N., Koster, J., Versteeg, R., Ora, I., Pajtler, K., Klein-Hitpass, L., Kuhfittig-Kulle, S., et al. (2009). Lysine-specific demethylase 1 is strongly expressed in poorly differentiated neuroblastoma: implications for therapy. Cancer Res. *69*, 2065–2071.
14. Karakaidos, P., Verigos, J., and Magklara, A. (2019). LSD1/KDM1A, a Gate-Keeper of Cancer Stemness and a Promising Therapeutic Target. Cancers *11*, 1821.
15. Maiques-Diaz, A., and Somervaille, T.C. (2016). LSD1: biologic roles and therapeutic targeting. Epigenomics *8*, 1103–1116.
16. Majello, B., Gorini, F., Saccà, C.D., and Amente, S. (2019). Expanding the Role of the Histone Lysine-Specific Demethylase LSD1 in Cancer. Cancers *11*, 324.
17. Perillo, B., Tramontano, A., Pezone, A., and Migliaccio, A. (2020). LSD1: more than demethylation of histone lysine residues. Exp. Mol. Med. *52*, 1936–1947.
18. Tsai, M.C., Manor, O., Wan, Y., Mosammaparast, N., Wang, J.K., Lan, F., Shi, Y., Segal, E., and Chang, H.Y. (2010). Long noncoding RNA as modular scaffold of histone modification complexes. Science *329*, 689–693.
19. Ding, J., Xie, M., Lian, Y., Zhu, Y., Peng, P., Wang, J., Wang, L., and Wang, K. (2017). Long noncoding RNA HOXA-AS2 represses P21 and KLF2 expression transcription by binding with EZH2, LSD1 in colorectal cancer. Oncogenesis *6*, e288.
20. Piao, L., Suzuki, T., Dohmae, N., Nakamura, Y., and Hamamoto, R. (2015). SUV39H2 methylates and stabilizes LSD1 by inhibiting polyubiquitination in human cancer cells. Oncotarget *6*, 16939–16950.
21. Han, X., Gui, B., Xiong, C., Zhao, L., Liang, J., Sun, L., Yang, X., Yu, W., Si, W., Yan, R., et al. (2014). Destabilizing LSD1 by Jade-2 Promotes Neurogenesis: An Antibraking System in Neural Development. Mol. Cell *55*, 482–494.
22. Yi, L., Cui, Y., Xu, Q., and Jiang, Y. (2016). Stabilization of LSD1 by deubiquitinating enzyme USP7 promotes glioblastoma cell tumorigenesis and metastasis through suppression of the p53 signaling pathway. Oncol. Rep. *36*, 2935–2945.
23. Wu, Y., Wang, Y., Yang, X.H., Kang, T., Zhao, Y., Wang, C., Evers, B.M., and Zhou, B.P. (2013). The deubiquitinase USP28 stabilizes LSD1 and confers stem-cell-like traits to breast cancer cells. Cell Rep. *5*, 224–236.
24. Deng, W.M., Althauser, C., and Ruohola-Baker, H. (2001). Notch-Delta signaling induces a transition from mitotic cell cycle to endocycle in Drosophila follicle cells. Development *128*, 4737–4746.
25. Lee, M.C., and Spradling, A.C. (2014). The progenitor state is maintained by lysine-specific demethylase 1-mediated epigenetic plasticity during Drosophila follicle cell development. Genes Dev. *28*, 2739–2749.
26. Margolis, J., and Spradling, A. (1995). Identification and behavior of epithelial stem cells in the Drosophila ovary. Development *121*, 3797–3807.
27. Nystul, T., and Spradling, A. (2007). An epithelial niche in the Drosophila ovary undergoes long-range stem cell replacement. Cell Stem Cell *1*, 277–285.
28. Sun, J., and Deng, W.M. (2005). Notch-dependent downregulation of the homeodomain gene cut is required for the mitotic cycle/endocycle switch and cell differentiation in Drosophila follicle cells. Development *132*, 4299–4308.
29. Sun, J., and Deng, W.M. (2007). Hindsight mediates the role of notch in suppressing hedgehog signaling and cell proliferation. Dev. Cell *12*, 431–442.
30. Rudolph, T., Yonezawa, M., Lein, S., Heidrich, K., Kubicek, S., Schäfer, C., Phalke, S., Walther, M., Schmidt, A., Jenuwein, T., and Reuter, G. (2007). Heterochromatin formation in Drosophila is initiated through active removal of H3K4 methylation by the LSD1 homolog SU(VAR)3-3. Mol. Cell *26*, 103–115.
31. Di Stefano, L., Ji, J.Y., Moon, N.S., Herr, A., and Dyson, N. (2007). Mutation of Drosophila Lsd1 disrupts H3-K4 methylation, resulting in tissue-specific defects during development. Curr. Biol. *17*, 808–812.
32. Eliazer, S., Shalaby, N.A., and Buszczak, M. (2011). Loss of lysine-specific demethylase 1 nonautonomously causes stem cell tumors in the Drosophila ovary. Proc. Natl. Acad. Sci. USA *108*, 7064–7069.
33. Kerenyi, M.A., Shao, Z., Hsu, Y.J., Guo, G., Luc, S., O'Brien, K., Fujiwara, Y., Peng, C., Nguyen, M., and Orkin, S.H. (2013). Histone demethylase Lsd1 represses hematopoietic stem and progenitor cell signatures during blood cell maturation. Elife *2*, e00633.
34. Rudolph, T., Beuch, S., and Reuter, G. (2013). Lysine-specific histone demethylase LSD1 and the dynamic control of chromatin. Biol. Chem. *394*, 1019–1028.
35. Shao, T.L., Ting, R.T., and Lee, M.C. (2022). Identification of Lsd1-interacting non-coding

RNAs as regulators of fly oogenesis. Cell Rep. *40*, 111294.
36. Hwang, W.W., Venkatasubrahmanyam, S., Ianculescu, A.G., Tong, A., Boone, C., and Madhani, H.D. (2003). A conserved RING finger protein required for histone H2B monoubiquitination and cell size control. Mol. Cell *11*, 261–266.
37. Bray, S., Musisi, H., and Bienz, M. (2005). Bre1 is required for Notch signaling and histone modification. Dev. Cell *8*, 279–286.
38. Weake, V.M., and Workman, J.L. (2008). Histone ubiquitination: triggering gene activity. Mol. Cell *29*, 653–663.
39. Shi, Y., Lan, F., Matson, C., Mulligan, P., Whetstine, J.R., Cole, P.A., Casero, R.A., and Shi, Y. (2004). Histone demethylation mediated by the nuclear amine oxidase homolog LSD1. Cell *119*, 941–953.
40. Forneris, F., Binda, C., Battaglioli, E., and Mattevi, A. (2008). LSD1: oxidative chemistry for multifaceted functions in chromatin regulation. Trends Biochem. Sci. *33*, 181–189.
41. Wood, A., Krogan, N.J., Dover, J., Schneider, J., Heidt, J., Boateng, M.A., Dean, K., Golshani, A., Zhang, Y., Greenblatt, J.F., et al. (2003). Bre1, an E3 ubiquitin ligase required for recruitment and substrate selection of Rad6 at a promoter. Mol. Cell *11*, 267–274.
42. Batta, K., Zhang, Z., Yen, K., Goffman, D.B., and Pugh, B.F. (2011). Genome-wide function of H2B ubiquitylation in promoter and genic regions. Genes Dev. *25*, 2254–2265.
43. Murawska, M., Schauer, T., Matsuda, A., Wilson, M.D., Pysik, T., Wojcik, F., Muir, T.W., Hiraoka, Y., Straub, T., and Ladurner, A.G. (2020). The Chaperone FACT and Histone H2B Ubiquitination Maintain S. pombe Genome Architecture through Genic and Subtelomeric Functions. Mol. Cell *77*, 501–513.e7.
44. Lee, J.S., Shukla, A., Schneider, J., Swanson, S.K., Washburn, M.P., Florens, L., Bhaumik, S.R., and Shilatifard, A. (2007). Histone crosstalk between H2B monoubiquitination and H3 methylation mediated by COMPASS. Cell *131*, 1084–1096.
45. Nakanishi, S., Lee, J.S., Gardner, K.E., Gardner, J.M., Takahashi, Y.h., Chandrasekharan, M.B., Sun, Z.W., Osley, M.A., Strahl, B.D., Jaspersen, S.L., and Shilatifard, A. (2009). Histone H2BK123 monoubiquitination is the critical determinant for H3K4 and H3K79 trimethylation by COMPASS and Dot1. J. Cell Biol. *186*, 371–377.
46. Shilatifard, A. (2012). The COMPASS Family of Histone H3K4 Methylases: Mechanisms of Regulation in Development and Disease Pathogenesis. Annu. Rev. Biochem. *81*, 65–95.
47. Kim, J., Guermah, M., McGinty, R.K., Lee, J.S., Tang, Z., Milne, T.A., Shilatifard, A., Muir, T.W., and Roeder, R.G. (2009). RAD6-Mediated Transcription-Coupled H2B Ubiquitylation Directly Stimulates H3K4 Methylation in Human Cells. Cell *137*, 459–471.
48. Ezhkova, E., and Tansey, W.P. (2004). Proteasomal ATPases link ubiquitylation of histone H2B to methylation of histone H3. Mol. Cell *13*, 435–442.
49. Gallego, L.D., Schneider, M., Mittal, C., Romanauska, A., Gudino Carrillo, R.M., Schubert, T., Pugh, B.F., and Köhler, A. (2020). Phase separation directs ubiquitination of gene-body nucleosomes. Nature *579*, 592–597.
50. Liu, Z., Oh, S.M., Okada, M., Liu, X., Cheng, D., Peng, J., Brat, D.J., Sun, S.Y., Zhou, W., Gu, W., and Ye, K. (2009). Human BRE1 Is an E3 Ubiquitin Ligase for Ebp1 Tumor Suppressor. Mol. Biol. Cell *20*, 757–768.
51. Chin, L.S., Vavalle, J.P., and Li, L. (2002). Staring, a novel E3 ubiquitin-protein ligase that targets syntaxin 1for degradation. J. Biol. Chem. *277*, 35071–35079.
52. Fu, J., Liao, L., Balaji, K.S., Wei, C., Kim, J., and Peng, J. (2021). Epigenetic modification and a role for the E3 ligase RNF40 in cancer development and metastasis. Oncogene *40*, 465–474.
53. Hirschi, A., Martin, W.J., Luka, Z., Loukachevitch, L.V., and Reiter, N.J. (2016). G-quadruplex RNA binding and recognition by the lysine-specific histone demethylase-1 enzyme. RNA *22*, 1250–1260.
54. Shi, Y.J., Matson, C., Lan, F., Iwase, S., Baba, T., and Shi, Y. (2005). Regulation of LSD1 histone demethylase activity by its associated factors. Mol. Cell *19*, 857–864.
55. Song, Y., Dagil, L., Fairall, L., Robertson, N., Wu, M., Ragan, T.J., Savva, C.G., Saleh, A., Morone, N., Kunze, M.B.A., et al. (2020). Mechanism of Crosstalk between the LSD1 Demethylase and HDAC1 Deacetylase in the CoREST Complex. Cell Rep. *30*, 2699–2711.e8.
56. Guida, M.C., Birse, R.T., Dall'Agnese, A., Toto, P.C., Diop, S.B., Mai, A., Adams, P.D., Puri, P.L., and Bodmer, R. (2019). Intergenerational inheritance of high fat diet-induced cardiac lipotoxicity in Drosophila. Nat. Commun. *10*, 193.

STAR★METHODS

KEY RESOURCES TABLE

REAGENT or RESOURCE	SOURCE	IDENTIFIER
Antibodies		
Guinea pig anti Lsd1	Dr. Michael Buszczak	*N/A*
Rabbit anti-GFP	Invitrogen	A11122; RRID:AB_221569
Rabbit anti-Bre1	This paper	N/A
Rabbit anti H3K27Me3	Cell signaling	#9733s; RRID:AB_2616029
Rabbit anti H3K4Me2	Millipore	#07-030; RRID:AB_310342
Rabbit anti H3K27Ac	Abcam	#ab4729; RRID:AB_2118291
Rabbit anti CoRest	Dr, Gail Mandel	*N/A*
Mouse anti Lsd1	Dr. Allan Spradling	*N/A*
Mouse anti α-tubulin	DSHB	#12G10; RRID:AB_2315509
Mouse anti-Cut	DSHB	2B10; RRID:AB_528186
Mouse anti-Hnt	DSHB	1G9; RRID:AB_528278
Goat anti-rabbit 488	Invitrogen	#A-11008; RRID:AB_143165
Goat anti-mouse 488	Invitrogen	#A-11001; RRID:AB_2534069
Goat anti-mouse 568	Invitrogen	#A-11004; RRID:AB_2534072
Chemicals, peptides, and recombinant proteins		
RNase cocktail Enzyme Mix	Invitrogen	Cat #: AM2286
RNase III	Invitrogen	Cat #: AM2290
RNasin ribonuclease inhibitor	Promega	Cat #: N2111
Rabbit IgG	Cell signaling	Cat #: 2729S
A/G beads Dynabeads	Pierece	Cat #: 53135
Mounting medium with DAPI	EMS	Cat #: 17989-20
MG132	Sigma-Aldrich	Cat #: 474787
Cycloheximide	Sigma-Aldrich	Cat #: C1988
Ubiquitin	BostonBiochem	Cat #: U-100At
ATP	Sigma-Aldrich	Cat #: A6419
Critical commercial assays		
Purelink RNA mini Kit	Invitrogen	Cat #: 12183018A
Biotin RNA Labeling kit	Roche	Cat #: 10999644001
RNAscope 2.5 HD Detection Reagent – RED	ACD	Cat #: 322360
ACD HybEZ Hybridization System	ACD	Cat #: 321461
Deposited data		
Data set of IgG-RIP and Bre1-RIP	NIH	GSE244906
Experimental models: Organisms/strains		
GMR10H05	*Bloomington Drosophila Stock Center*	*BDSC:#48276*
D. melanogaster: hs-FLP; tub > CD2 > Gal4 N/A UAS-GFP/CyO	Laboratory of A. Spradling	*N/A*
D. melanogaster: P{ry[+t7.2]=PZ}Bre1[01640] ry[506]/TM6B ry[CB] Tb[+]	*Bloomington Drosophila Stock Center*	*BDSC:#11541*
D. melanogaster: RNAi of Bre1: y[1] sc[*] v[1]; P{y[+t7.7] v[+t1.8] = TRiP.JF01309} attP2	*Bloomington Drosophila Stock Center*	*BDSC:#31351*

(*Continued on next page*)

Continued

REAGENT or RESOURCE	SOURCE	IDENTIFIER
D. melanogaster: RNAi of Bre1: y[1] v[1]; P{y[+t7.7] v[+t1.8] = TRiP.JF02853} attP2	*Bloomington Drosophila Stock Center*	*BDSC:#28019*
D. melanogaster: RNAi of gzl: y[1] sc[*] v[1] sev[21]; P{y[+t7.7] v[+t1.8] = TRiP.HMS05370} attP40	*Bloomington Drosophila Stock Center*	*BDSC:#64034*
D. melanogaster: RNAi of Hecw: y[1] sc[*] v[1] sev[21]; P{y[+t7.7] v[+t1.8] = TRiP.HMC03322} attP40	*Bloomington Drosophila Stock Center*	BDSC:#51767
D. melanogaster: RNAi of Hecw: y[1] v[1]; P{y[+t7.7] v[+t1.8] = TRiP.GLC01831} attP2/TM3, Sb[1]	*Bloomington Drosophila Stock Center*	BDSC:#55214
D. melanogaster: RNAi of HUWE1: : y[1] sc[*] v[1] sev[21]; P{y[+t7.7] v[+t1.8] = TRiP.HMS01604} attP40	*Bloomington Drosophila Stock Center*	BDSC:#36714
D. melanogaster: RNAi of HUWE1: y[1] sc[*] v[1] sev[21]; P{y[+t7.7] v[+t1.8] = TRiP.HMS01605} attP40	*Bloomington Drosophila Stock Center*	BDSC:#36715
D. melanogaster: RNAi of mus302: y[1] v[1]; P{y[+t7.7] v[+t1.8] = TRiP.HMJ23940} attP40/Cyo	*Bloomington Drosophila Stock Center*	BDSC:#62460
D. melanogaster: RNAi of Prp191: y[1] sc[*] v[1] sev[21]; P{y[+t7.7] v[+t1.8] = TRiP.HMS00652} attP2	*Bloomington Drosophila Stock Center*	BDSC:#32865
D. melanogaster: RNAi of Mkrn1: y[1] sc[*] v[1] sev[21]; P{y[+t7.7] v[+t1.8] = TRiP.HMS01363} attP2	*Bloomington Drosophila Stock Center*	BDSC:#34373
D. melanogaster: RNAi of Mkrn1: y[1] v[1]; P{y[+t7.7] v[+t1.8] = TRiP.GL01521} attP2	*Bloomington Drosophila Stock Center*	BDSC:#43178
D. melanogaster: hs-FLP/+; FRT80B, ubi-GFP/ FRT80B, +; LINR-2$^{\Delta}$	*This paper*	
D. melanogaster: LINR-1$^{\Delta}$	Laboratory of M. Lee (Shao et al., 2022)[35]	*N/A*
D. melanogaster: LINR-2$^{\Delta}$	Laboratory of M. Lee (Shao et al., 2022)[35]	*N/A*
D. melanogaster: LINR-3/4$^{\Delta}$	Laboratory of M. Lee (Shao et al., 2022)[35]	*N/A*
Oligonucleotides		
GST_Lsd1_full_EcoRI_fw: 5′-CTGAATTCAGATGAAACCCACCCAGTTCG-3′	*This paper*	*N/A*
GST_Lsd1_full_NotI_Re: 5′-GAGCGGCCGCTTACTGTAGCTCCGTAGAGTCG-3′	*This paper*	*N/A*
LD45081 (Lsd1 cDNA)	Drosophila Genomics Resource Center	RRID:DGRC_5248

RESOURCE AVAILABILITY

Lead contact

Further information and requests for resources and reagents should be directed to and will be fulfilled by the Lead Contact, Ming-Chia Lee (lee.mingchia@nycu.edu.tw).

Materials availability

All unique reagents generated in this study are available form the lead contact without restriction.

Data and code availability

- RIP-seq data have been deposited at GEO (GSE244906) and are publicly available as of the date of publication. Accession numbers are also listed in the key resources table. Data reported in this paper will be shared by the lead contact upon request.
- No code was generated in this study.
- Any additional information required to analyze the data reported in the paper is available from the lead contact upon request.

EXPERIMENTAL MODEL AND STUDY PARTICIPANT DETAILS

Drosophila melanogaster (Fruit fly)

Flies were reared under standard lab conditions at 25°C. Fly stocks used in this study were mostly acquired from Bloomington *Drosophila* Stock Center and Vienna *Drosophila* Resource Center. *Oregon-R* was used as control strain in this study. *R10H05-Gal4 (BDSC#48276)*; *hs-FLP*; tub>CD2>Gal4, UAS-GFP (gift of A. Spradling); *Bre1* RNAi lines *(#1: BDSC# 31351, #2: BDSC#28019); gzl RNAi (BDSC#64034); Hecw RNAi (BDSC#51767 and BDSC#55214); HUWE1 RNAi (BDSC#36714 and BDSC#36715); mus302 RNAi (BDSC#62460); Prp191 RNAi (BDSC#32865); Mkrn1 RNAi (BDSC#34373 and BDSC#43178). Bre1* mutant line *(BDSC#11541: P{PZ}Bre^{101640}, ry^{506}/TM6B, ry^{CB})*. Mutant lines of *LINRs* (i.e., *LINR-1$^{\Delta}$* , *LINR-2$^{\Delta}$* and *LINR-3/4$^{\Delta}$*) and *hs-FLP/+; FRT80B, ubi-GFP/ FRT80B, +; LINR-2$^{\Delta}$)* were generated in our lab as previously indicated.[35] Adult female flies of indicated genotypes were used in this study. For collecting ovarian lysate used in biochemical assays, young adult females (<12hr post eclosion) were collected. For immunostaining and phenotypic analyses, 4-7 days old adult females were collected and fed with wet yeast for at least 2 days prior to dissection.

METHOD DETAILS

Fly husbandry

Flies were reared under standard lab conditions at 25°C. For collecting ovarian lysate used in biochemical assays, young adult females (<12hr post eclosion) containing a relative higher proportion of follicle progenitors were collected. For immunostaining and phenotypic analyses, 4-7 days old adult females were collected and fed with wet yeast for at least 2 days prior to dissection. For RNAi experiments, selected Gal4 drivers were crossed with specific RNAi lines. For better RNA interference efficiency, F1 larvae were shifted to 29°C at late larval stage 3. Similarly, 4-7 days old adult F1 females were collected and fed with wet yeast for at least 2 days prior to dissection.

Generation of anti-Bre1 antisera

The rabbit polyclonal antibody recognizing a unique *Drosophila* Bre1 peptide (*CNVAIKEENHISAED*) was generated using GenScript service. The specificity of antibody was tested by ELISA against its epitope. When used for immunoblotting in ovarian lysate, this antibody recognizes a major band of ~120 KD, close to the predicted size of fly Bre1 (119.09 KD). Moreover, the signal of this major band is decreased when the antibody was used to blot the ovarian lysate prepared from Bre1 mutant (*P{PZ}Bre^{101640}, ry^{506}/TM6B, ry^{CB}*) ovaries, indicating that this Bre1 antibody specifically recognize the endogenous ovarian Bre1 protein. In this study, this rabbit anti-Bre1 polyclonal antibody (1:1000) was used in Western Blotting, Co-IP, and RIP experiments.

In situ hybridization

BaseScope™ (ACD) probes were designed targeting specific sequences of Lsd1 (i.e., 3x ZZ probes were designed to target 436-557 of NM_140937.3). Ovaries were dissected from female flies for RNA *in situ* hybridization as previously described[56] and the manufacture's protocol was followed. Images were acquired using an Apotome.2 (Zeiss), ZEN 2.3 pro software and later analyzed using both Metamorph and ImageJ.

Immunoprecipitation and Western Blotting

Immunoprecipitation and Western Blot were performed as described previously.[35] Briefly, for each set of immunoprecipitation experiment, 0.3-0.5 ml of ovarian lysate was prepared from ~150 pairs of young fly ovaries. Specific volume of lysate was set aside for preparing loading input (5%-10%). Each IP reaction was set up using 150-200 μl of lysate by adding 5 μg of selected antibodies (Guinea pig anti-Lsd1 or Rabbit anti-Bre1). IP was performed on nutator at 4°C for overnight, and then pulled down by pre-washed A/G beads (Pierece #53135). IP samples were then washed and prepared for SDS PAGE and Western Blotting. For determining whether Lsd1 protein expression is regulated post-translationally, dissected ovaries were kept in PBS and incubated with cycloheximide or MG132 at room temperature for the indicated period of time. While 200 μM of cycloheximide was used to block protein syntheses, 10 μM of MG132 was use inhibit proteasome activity. Antibodies used for IP are guinea pig anti-Lsd1 antibody (a gift from Dr. Michael Buszczak, 1:1000) and rabbit anti-Bre1 antibody (1:1000). Antibodies used for immunoblotting include Rabbit guinea pig anti-Lsd1 antibody (1:1000), rabbit anti-ubiquitin (Abcam#19247, 1:1000), rabbit anti-Bre1 antibody (1:1000) and mouse anti-α-tubulin (DHSB#12G10, 1:200). For determining if dsRNAs are involved in Lsd1-Bre1 binding, 10μl of RNase III (Invitrogen#AM2290) was added into the IP reactions (at 37°C for 30 minutes) for dsRNA hydrolysis. For examining if the presence of *LINR-1* or *LINR-2* transcripts affects the binding between Bre1 and Lsd1, half microgram of specific biotinylated *LINR* transcripts was added into Bre1-IP reaction to test if the amount of Lsd1 protein pulled down by Bre1-IP is affected. Biotin-labelled *LINRs* were *in vitro* transcribed with Biotin RNA Labeling kit (Roche #10999644001) at 37°C for 30 minutes, purified (Purelink RNA mini-Kit; Invitrogen #12183018A) and then fold (RNAs in RNA structure buffer [10 mM Tris pH 7, 0.1 M KCl, 10 mM $MgCl_2$] were heated to 90°C for 2 minutes and then gradually cooled down to allowing folding).

Immunostaining and Microscopy

Ovaries were dissected in ice-cold PBS solution. Dissected ovaries were fixed in 4% paraformaldehyde in 1x PBS for 15 minutes at room temperature. Primary antibodies were added and then incubated for overnight at 4°C. Antibodies used in this study are rabbit anti-GFP

(Invitrogen #A11122, 1:1000), mouse anti-GFP (Invitrogen #A11120, 1:1000), rabbit anti-H3K4Me2 (Millipore #07-030, 1:1000), rabbit anti-H3K27Ac (Abcam #ab4729, 1:1000), rabbit anti-H3K27Me3 (Cell signaling #9733, 1:1000), mouse anti-Lsd1 (1:2500,[25] mouse anti-Hnt (DSHB #1G9, 1:20) and mouse anti-Cut (DSHB #2B10, 1:25). Secondary antibodies used are goat anti-rabbit 488 (Invitrogen #A11008, 1:500), goat anti-mouse 488 (Invitrogen #A11001, 1:500), goat anti-mouse 568 (Invitrogen #A11004, 1:500) and goat anti-rabbit 568 (Invitrogen #A11011, 1:500). Stained ovaries were mounted in mounting medium with DAPI (EMS#17989-20) on glass slides. Images were taken on Zeiss Axio Imager 2/Apotome.2 microscope and processed with ImageJ software. As previously described, the number of follicle cells was quantified by taking pictures of stage 10 egg chambers and counting the number of nuclei (based on DAPI signals) per side using ImageJ software.[25]

Clonal generation and measurements

For generating FLO clones, female flies of *hs-FLP*; tub>CD2>Gal4/+, UAS-GFP/+ or *hs-FLP*; tub>CD2>Gal4/+, UAS-GFP/Bre1$^{RNAi\#1\ or\ \#2}$ were collected and subjected to 30 minutes of heat shock at 37°C twice a day for two days. Then the flies were kept at 29°C and fed with wet yeast daily for 3 days before dissection. The ovaries were dissected and fixed as the procedures described above and prepared for immunostaining. To assess the effects of *Bre1* knockdown on Lsd1 protein expression of follicle progenitors, stage 3-7 egg chambers containing one GFP+ FLO clone were selected for further analysis. Potential signal variations among clones resulting from the processes of immunostaining and image acquisition were overcome by normalizing the clonal measurements of nuclear DPAI or Lsd1 signal (GFP+ *Bre1*-KD cells) to the corresponding neighboring GFP negative (GFP-) cells. Specifically, the normalized DAPI and Lsd1 intensities ($DAPI_{GFP+}/DAPI_{GFP-}$ and $Lsd1_{GFP+}/Lsd1_{GFP-}$) were used to reflect the corresponding clonal changes. The integrated intensity of the DAPI signal was measured to indicate cellular DNA content and no clonal changes of DNA content were observed in the 40 Bre1$^{RNAi\#1}$ FLO clones and 36 Bre1$^{RNAi\ \#2}$ FLO clones. Conversely, the integrated intensity of the Lsd1 signal was measured to infer the amount of cellular Lsd1 protein and about two-fold increase in clonal accumulation of Lsd1 protein was observed among the 40 Bre1$^{RNAi\#1}$ FLO clones and 36 Bre1$^{RNAi\ \#2}$ FLO clones.

RNA-Immunoprecipitation (RIP)

RIP experiments were performed as described previously.[35] Briefly, 150-200 pairs of ovaries were dissected from young female flies (<12 hours post eclosion) in ice-cold PBS solution and then transferred into RIP buffer (300-500 μl; 150 mM KCl, 25 mM Tris pH 7.4, 0.5 mM DTT, 0.5% NP40, 1 mM PMSF and protease Inhibitor [Roche, #11836170001]). In RIP buffer, ovaries were mechanically sheared using a dounce homogenizer with 15–20 strokes and then incubated on ice for 15 minutes. Then, cell membrane and debris were pelleted by centrifugation at 12,500 RPM at 4°C for 20 min. Collected supernatant was then supplemented with RNasin (ribonuclease inhibitor [Promega #N2111]) as ovarian lysate. Lysate was then split into two parts for adding either control or experimental antibodies. RIP samples were then incubated at 4°C for overnight. Specifically, for Lsd1-RIP experiments, rabbit anti-GFP (Invitrogen #A-11122) and guinea pig anti-Lsd1 (a gift from Dr. Michael Buszczak, 1:1000) were used. For Bre1-RIP experiments, rabbit anti-GFP (Invitrogen #A-11122) and rabbit anti-Bre1 were used. Then, prewashed protein A/G Dynabeads (Pierece #53135) was added into each IP reaction and incubate for 2 hours at room temperature. After wash, RNAs were extracted from the Dynabeads using 1ml Trizol/Chloroform followed by Purelink RNA mini-Kit (Invitrogen #12183018A). Extracted RNAs from RIP samples then underwent cDNA library construction for Next Generation Sequencing. Raw (single end) reads were then subjected to Tophat (bowtie2)> Cufflinks pipeline for transcriptome assembly and for estimating abundance of individual transcripts (RPKM). Release 6 (dm6) was used as the reference genome. For the three paired RIP-Seq experiments, each of 50-80 million reads was obtained to make sure sufficient coverage of individual RIP outputs.

Generation and purification of GST-LSD1 recombinant protein

The amplified Lsd1 cDNA clone LD45081 (BDGP) was used as the template for amplifying Lsd1 cDNA sequence (a 2673 bp DNA fragment). The PCR primers utilized are listed as below:

GST_Lsd1_full_EcoRI_fw: 5′-CTGAATTCAGATGAAACCCACCCAGTTCG-3′

GST_Lsd1_full_NotI_Re: 5′-GAGCGGCCGCTTACTGTAGCTCCGTAGAGTCG-3′

The Lsd1 cDNA sequence (PCR product) was digested with EcoR I and Not I restriction enzymes and then cloned into pGEX-4T-2 plasmid for generating pGEX-4T-2_Lsd1 construct. pGEX-4T-2_Lsd1 was validated by sequencing and then transformed into BL21(DE3) pLysS Competent Cells (Promega# L1195) for expression and purification of recombinant GST-Lsd1 protein. A single bacteria colony of pGEX-4T-2_Lsd1 transformants was inoculated in ampicillin (50μg/ml) containing LB medium and grow at 37°C for overnight. The overnight bacteria culture was diluted (1:20) in LB medium (200 ml) to grow until the OD_{600} reaches 1.0 when IPTG was added into the culture (1mM) to induce the expression of recombinant GST-Lsd1. The culture was incubated at 250 RPM/37°C for 4 hours, and span at 3500xg/4°C for 10 minutes to pellet bacteria. Collected bacteria pellet was resuspended in 2 ml cold lysis buffer (PBS with 1% Triton and protease inhibitors [Roche, #11836170001]) and then lysed with ultra-sonication (20-second bursts with 30 second rests between pulses for three to five minutes). The sonicated lysate was centrifuged the at 13500 RPM at 4°C for 15 minutes. Supernatant was collected for recombinant protein purification. Prewashed glutathione-agarose beads (Cytiva #274671) were added into the supernatant collected (100μL of 50% slurry for supernatant from 50mL culture) and incubate at 25°C for 3 hours. Then, GST-Lsd1 bound agarose beads were washed 3 times with lysis buffer and 3 times in washing buffer (50 mM Tris, pH 7.4, 1 M NaCl, 1 mM EDTA) and then twice with ubiquitination buffer (20 mM Tris, pH 7.4, 5 mM $MgCl_2$, 0.5 mM EDTA) before using in the ubiquitination assays.

Ubiquitination assay

Purified GST-Lsd1 proteins were prepared as described in the "***purification of GST-LSD1***" session. Individual microcentrifuge tubes containing purified GST-Lsd1 (10μl), HA ubiquitin (0.5 ug; R&D system #U110) in ubiquitin buffer (20 mM Tris, pH 7.4, 5 mM $MgCl_2$, 0.5 mM EDTA, 2mM ATP, 10μM MG132) was then added with 25 μl of water, ovarian lysate, or immunoprecipitated Bre1 complex (Bre1-IP) respectively. After incubating at 25°C for 3.5 hours, ubiquitin conjugation reaction products (ubiquitinated Lsd1) were assayed by SDS-PAGE and Western blot. Ovarian lysate and Bre1-IP were prepared as previously described.[35] Briefly, ovarian lysate (100 μl) was prepared from ~100 pairs of young fly ovaries. While 30 μl of ovarian lysate was set aside for examine its ability to induce GST-Lsd1 ubiquitination, the remaining 70 μl ovarian lysate was used to prepare Bre1-IP and the lysate depleted with Bre1 protein complexes (Bre1_del). The lysate incubated with 2.5 μg of rabbit anti-Bre1 antibody and prewashed protein A/G magnetic beads (40 μl Pierce#88802) at 25°C for 2 hours, and then put on a magnetic rack to obtain Bre1-bound AG beads and the Bre1-del lysate. Bre1-bound AG beads (Bre1-IP) were then washed for 3 time in washing buffer (50 mM Tris, pH 7.4, 1 M NaCl, 1 mM EDTA) before being used for the ubiquitination assay.

QUANTIFICATION AND STATISTICAL ANALYSIS

The effects of MG132 application on ovarian Lsd1 protein expression were quantified by measuring the integrated intensity of Lsd1-immuno blots (three independent experiments) of lysates prepared from ovaries treated with or without MG132 for two hours. Student's t-test was used to examine whether MG132 treatment leads to elevated Lsd1 protein expression. * $p<0.05$.

The effects of *Bre1* knockdown on Lsd1 protein expression were assessed by calculating 'Clonal Lsd1 accumulation' (see details in the section on Clonal generation and measurements). Briefly, the integrated intensities of the Lsd1 signal (or DAPI signal) were measured in individual Bre1 KD clones and corresponding control neighboring cells. Student's t-test was used to examine 'Clonal Lsd1 accumulation' while paired student's t-test was used to examine the differences in Lsd1 intensity among individual clones. Student's t-test was utilized to examine whether DNA contents were altered in Bre1 KD clones. ** $p<0.01$; N.S. non-significant.